Influence of non-equilibrium on disturbance waves passing through a planar shock

By C. Stemmer†, N. A. Adams† AND N. N. Mansour

The present study investigates the behavior of harmonic waves passing through a strong shock in the presence of chemical reactions and thermal non-equilibrium. At a hypersonic Mach number (M=20), a planar sinusoidal wave is excited at the inflow boundary of a steady strong planar shock system. The amplitude and wave length of the disturbance is altered as it passes through the shock. As a reference case, ideal gas conditions are calculated. The disturbance amplitude and wavelength both decrease by a factor of 1.6 for the frequency of 100 kHz. In a first stage, the behavior in the presence of chemical reactions (equilibrium) is shown. For the equilibrium case, the amplitude decreases twice as much as for the ideal gas case (by 3.3) and the wave length is decreased by 2.3. The non-equilibrium case exhibits contrary behavior. The amplitude rises by 5.5 and the wave length increases by a factor of 1.2. This shows the direct influence of non-equilibrium on the amplitudes and wave lengths of disturbance waves passing through a shock.

1. Introduction

Hypersonic re-entry vehicles from low-earth orbit (LEO) enter the atmosphere at speeds of about 7.8 km/s, which is in the Mach number range of about 25. In the upper layer of the atmosphere (h>100 km), free molecular flow is present. As the vehicle gets slowed down on its path toward Earth, the density increases such that continuum approaches are justified. The Mach number in an altitude of about 80–50 km is still about 20, which leads to high degrees of non-equilibrium (chemically and thermally) behind strong shock waves (see also Miller 2005). As the density becomes higher, the question of transition of the laminar flow to a turbulent state arises (Stemmer 2005). As the transition process involves the exponential amplification of certain waves and resonance between a group of waves in the late stages of transition, the influence of small shocks inside the boundary layer on the development of waves and their resonances has to be investigated. The shocks inside the boundary layer (also called shocklets) are a result of the velocity disturbances of non-linear amplitudes in high-speed boundary layers. As the shocks are the source of non-equilibrium, the present work attempts to break down that complex process which usually involves a whole spectrum of disturbance waves into a model problem.

The present work focuses on the behavior of solitary waves as they pass through a strong shock wave. Single waves have been used for the direct numerical simulations (DNS) to identify individual changes in frequency and wave length as well as amplification or attenuation in amplitude. If one were to investigate a white noise spectrum, only global conclusions would be possible. The investigated frequencies lie in the frequency domain, where instabilities occur for the current flow conditions.

The behavior of isotropic turbulence in the presence of a weak shock ($1.05 < M <$

† Lehrstuhl für Aerodynamik, Technische Universität München, Germany

1.2) for a thermal and chemical perfect gas has been investigated by Lee, Lele and Moin (1993). They found that turbulence was enhanced during interaction with a shock wave as the turbulent kinetic energy and transverse velocity components were amplified. The turbulent length scales were decreased. A local rapid increase of turbulent kinetic energy just downstream of the shock was also seen.

In a study extending the investigation to strong shocks originating from higher Mach-number flows, the increase of the turbulent kinetic energy saturated for M>3 (Lee, Lele and Moin (1997)).

Mahesh, Lee, Lele and Moin (1995) found distinct differences between the interaction of a vortical field (as in the studies of Lee *et al.* (1993)) with a shock compared to acoustic wave interaction with the shock. A decrease of kinetic energy from the acoustic waves due the interaction with a weak shock wave ($1.25 < \mathrm{M} < 1.8$) was observed. But at higher Mach numbers exceeding 3, the behavior was reversed and an increase in kinetic energy was observed. This was accompanied by a generation of vortical disturbances through the interaction. This lead to an increase of the far-field kinetic energy with higher Mach numbers.

Work devoted to study the interaction of entropy fluctuations in the presence of vortical fluctuations with shock waves for the range of $1.25 < \mathrm{M} < 1.8$ by Mahesh, Lele and Moin (1997) show a dependency of the behavior on the correlation of the two disturbances. A positive correlation between u' and T' has a suppressing effect on the amplification, whereas a negative correlation can be found to increase the amplification of the turbulent kinetic energy, vorticity and thermodynamic fluctuations.

Using these findings as a base, we investigated the role of chemical non-equilibrium on the aforementioned results.

2. Methodology

The present study was conducted using DNS with the NSMB code Vos *et al.* (1998), Vos, Duquesne, Lee (1999). NSMB is a finite volume higher-order method solving the Navier-Stokes equations capable of handling equilibrium, chemical non-equilibrium and chemical and thermal non-equilibrium. The method can handle shocks through an upwind discretization scheme.

A planar shock wave satisfying the Rankine-Hugoniot relations was prescribed as an initial solution and the numerical solution was iterated until it reached a steady state. In a second step, time-periodic fluctuations at the inflow boundary were prescribed and the simulation was continued until it became periodic in the solution. The disturbances introduced were of different nature.

Three different cases are presented here. For reference reasons, a perfect gas solution (Case I) is presented although the conditions would not allow for that in a real flow. The temperatures of more than 20,000 K behind the shock are unrealistic without the consideration of dissociation and recombination.

In Case II, chemical equilibrium is assumed where the chemical reaction rates are assumed to exhibit a time scale that tends to infinity thus assuring local equilibrium conditions for the respective temperatures. Case III uses chemical non-equilibrium where the speed of the chemical reaction rates is in the same order of magnitude as the flow time scale. Thus, the shock is a source of non-equilibrium and downstream of the shock, the chemical concentrations change as the flow evolves (see fig. 1, discussed in the results section)

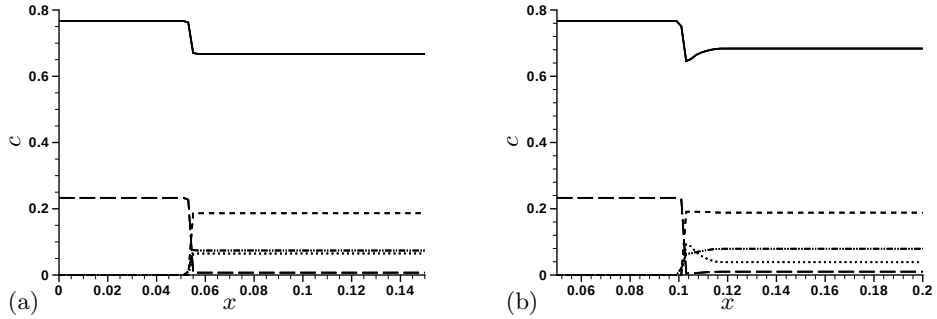

FIGURE 1. Species concentrations for (a) Case II and (b) Case III.
N_2: ——— ; N: ····· ; NO: —·—·— ; O_2: — — — ; O: — — —

For the inflow conditions, a M=20 flow at $T_\infty = 270.65$ K and $p_\infty = 101325$ N/m^2 was assumed. This amounts to a speed of $U_\infty = 6596$ m/s. For Case II and Case III, an initial concentration of the species of $c_{N2} = 0.767$ and $c_{O2} = 0.233$ was given.

3. Results

3.1. *Basic shock properties*

The perfect-gas shock solution satisfies the Rankine-Hugoniot relations as well as the ideal-gas equation

$$p = \rho R T,$$

where p is the pressure, ρ is the density, T is the temperature and the ideal gas constant is $R = 287$ J/(kg K).

For Case I, the temperature after the shock increases to $T_2 = 21,306.1$ K, the pressure to $p_2 = 4.727 \cdot 10^7$ N/m^2 and the density to $\rho = 7.73$ Kg/m^3.

For Case II, the chemical reactions (mostly the dissociation of oxygen and the buildup of nitric monoxide (NO); see fig. 5) take energy out of the flow and the temperature behind the shock increases to only $T_2 = 7,887.1$ K. The density increases to $\rho = 14.53$ Kg/m^3 and the pressure increases only to $p_2 = 4.07 \cdot 10^7$ N/m^2. As the exact chemical composition behind the shock is unknown at the beginning of the steady shock simulations, one starts with the ideal-gas simulation. Therefore a transient period with the shock moving is experienced. The simulations for Case II are in a moving frame of reference that moves at $u_s = 1070.535 m/s$, which has to be added to the shown velocities in the fig. 3 and 4.

The non-equilibrium case (Case III) exhibits thermodynamic properties that are in the same range once they reach a steady value. The concentrations change downstream of the shock (see fig. 5). It takes about $\Delta x = 0.02$ m until the equilibrium state (Case II) is reached again.

3.2. *Disturbance development*

The disturbance considered is an entropic disturbance, i.e., the pressure remains constant and the density disturbance satisfies the following relation

$$\rho' = \rho_\infty (\gamma - 1) \cdot M^2 \cdot \frac{u'}{U_\infty}.$$

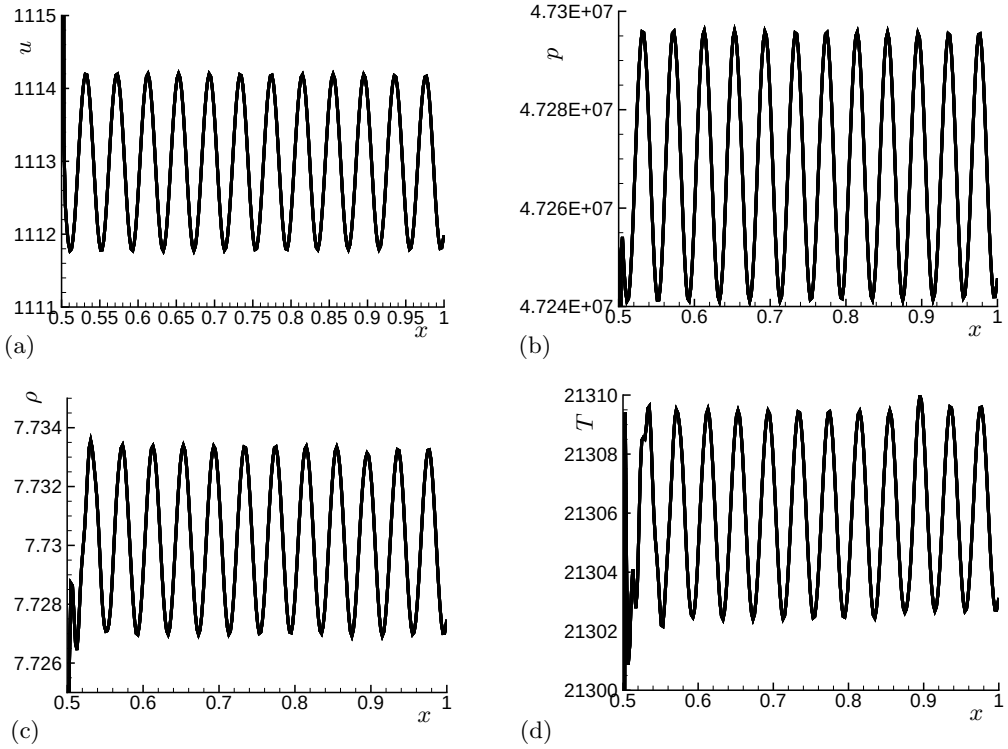

FIGURE 2. Case I: disturbance evolution for an entropic disturbance after the shock. (a) velocity u, (b) pressure, (c) density ρ, (d) temperature T.

The frequency chosen was F=100kHz and the velocity disturbance level was at $A_u = 0.5\%$.

For the ideal gas case (Case I), the disturbance development after the shock at $x = 0.5m$ is shown in fig. 2 (the velocity (subfigure a), pressure (subfigure b), density (subfigure c) and temperature (subfigure d) are presented). The entropic disturbance shows a harmonic behavior after it passes through the shock. The pressure also shows small oscillations (not the scale in fig. 2d) that indicate an acoustic disturbance being generated through the interaction of the entropic disturbance with the shock. Note that the amplitudes remain constant and no dissipation from the numerical scheme used is noticeable.

As the disturbance goes through the shock, the reference conditions change to the conditions after the shock. In absolute numbers, the disturbance amplitudes decrease. The relative disturbance velocity amplitudes (the reference is the local $\bar{u}$) decrease for the ideal gas case (Case I) by a factor of 1.6 and by the same factor in wavelength.

For the equilibrium case (Case II), the resulting instantaneous distribution after the disturbance input at the inflow boundary and before the shock at $x = 0.075$ is presented in fig. 3.

The evolution of the disturbance amplitudes after the shock is shown in fig. 4. It is obvious that the harmonic nature as in the ideal gas case is lost and at least two different types of disturbances with very close wave lengths are present. The pressure fluctuation is not small; an acoustic disturbance has clearly developed. The relative disturbance

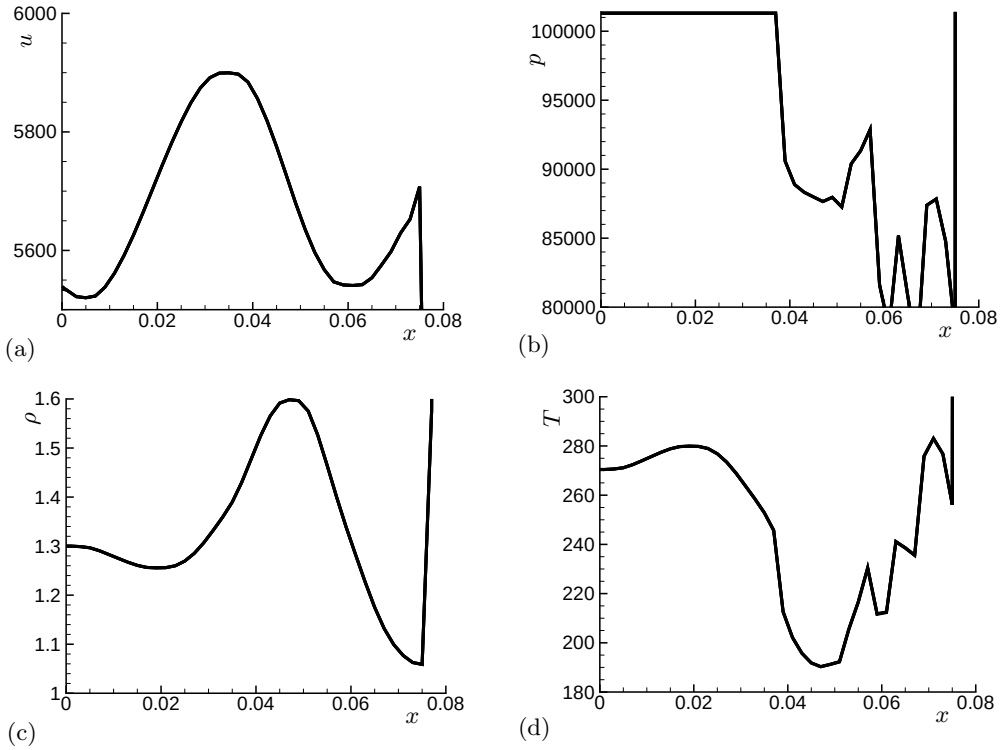

FIGURE 3. Case II: disturbance evolution for an entropic disturbance before the shock. (a) velocity u, (b) pressure, (c) density ρ, (d) temperature T.

velocity amplitudes decrease for the equilibrium case (Case II) by a factor of 3.3 and by a factor of 2.3 in wavelength.

The influence of the linear disturbance on the concentrations is as expected (see fig. 5a). The disturbances appear as small oscillations in the concentrations. Most noticeable is the oscillation of the molecular nitrogen (solid line) because it has the highest concentration. The change in molecular nitrogen leads to a change in atomic nitrogen concentration (dotted line). As molecular oxygen (long dashes) is fully dissociated, the nitric oxygen concentration (dash-dot-dotted) and the atomic oxygen are the most strongly influenced by the disturbances.

For the same disturbance, the non-equilibrium case (Case III) exhibits very different properties. Before the shock, the disturbance is as presented in fig. 6.

The disturbance velocity amplitude increases by a factor of 5.5 and the wave length increases by a factor of 1.2 behind the shock. The disturbance development downstream of the shock for Case III is presented in fig. 7. Only one to two disturbance wave lengths are shown since the overall level of the respective property moves out of the shown range due to the change of the thermodynamic properties and chemical species.

The development of the species concentrations downstream of the shock is shown in fig. 5b. The small oscillations in the concentrations can be noticed in Case III as in the equilibrium case, but the levels reached further downstream of the shock are different after the non-equilibrium effect of the shock has subsided. This is most noticeable in the concentration of atomic nitrogen (dashed line), as it drops slowly to about half the level

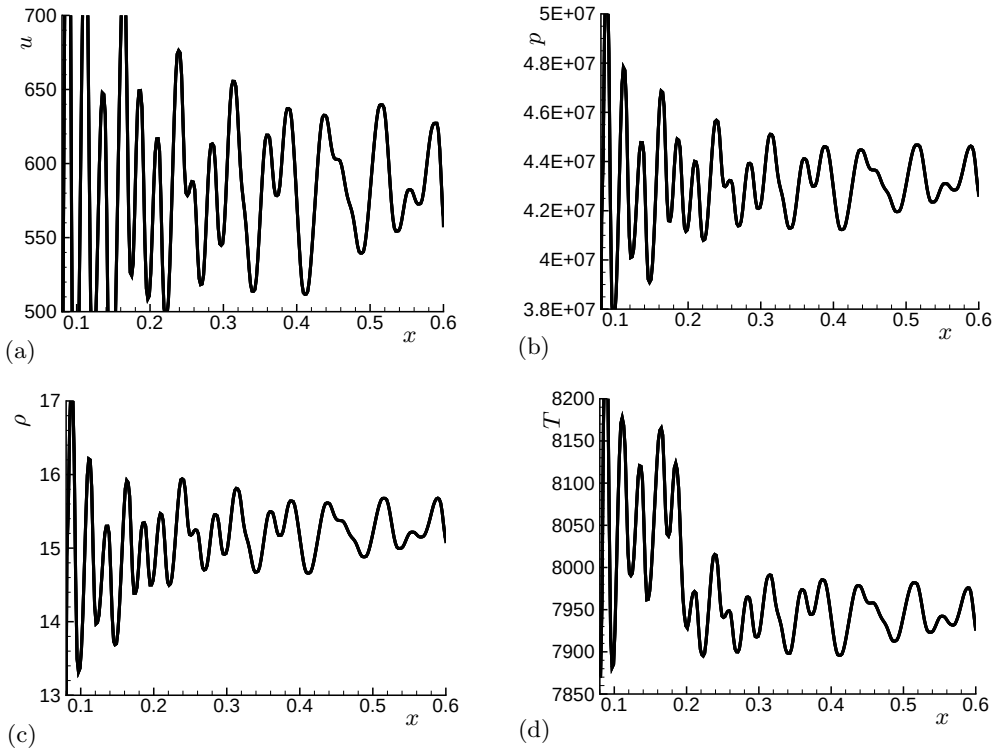

FIGURE 4. Case II: disturbance evolution for a entropic disturbance after the shock. (a) velocity u, (b) pressure, (c) density ρ, (d) temperature T.

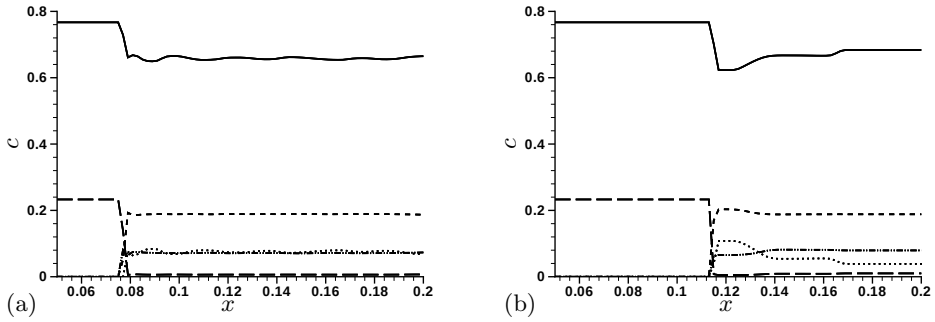

FIGURE 5. species concentrations for the disturbed (a) Case II and (b) Case III. N_2: ——— ; N: ····· ; NO: —·—·— ; O_2: — — — ; O: – – – –

compared to Case II). The oscillations can also be observed in all concentrations just downstream of the shock.

4. Conclusions

The behavior of harmonic entropic disturbances as they move through a planar shock wave are presented in this work. Three different cases are investigated. First, for reference

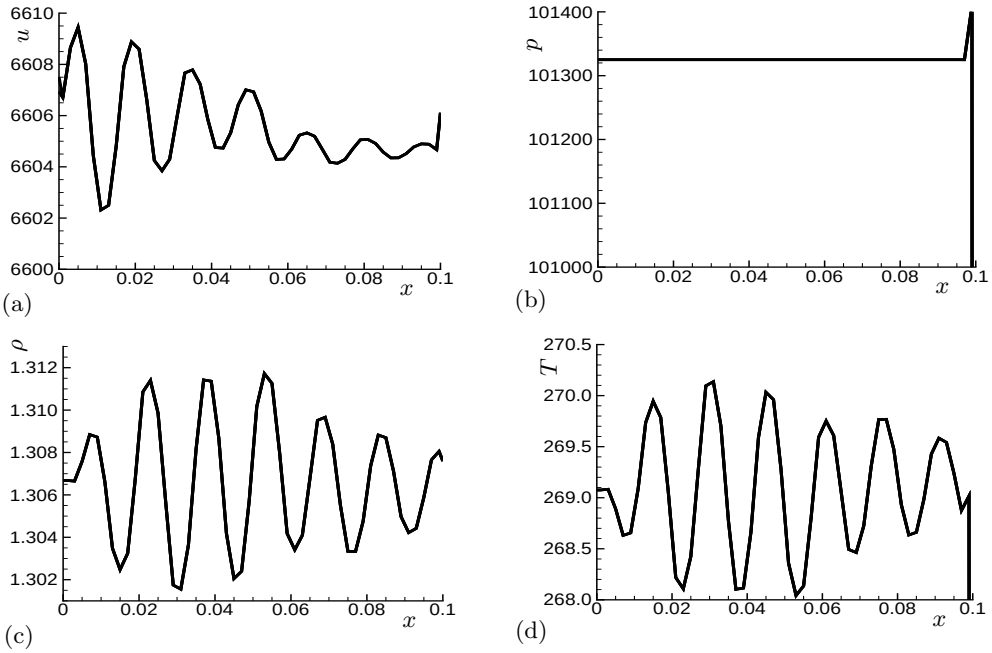

FIGURE 6. Case III: disturbance evolution for a entropic disturbance before the shock. (a) velocity u, (b) pressure, (c) density ρ, (d) temperature T.

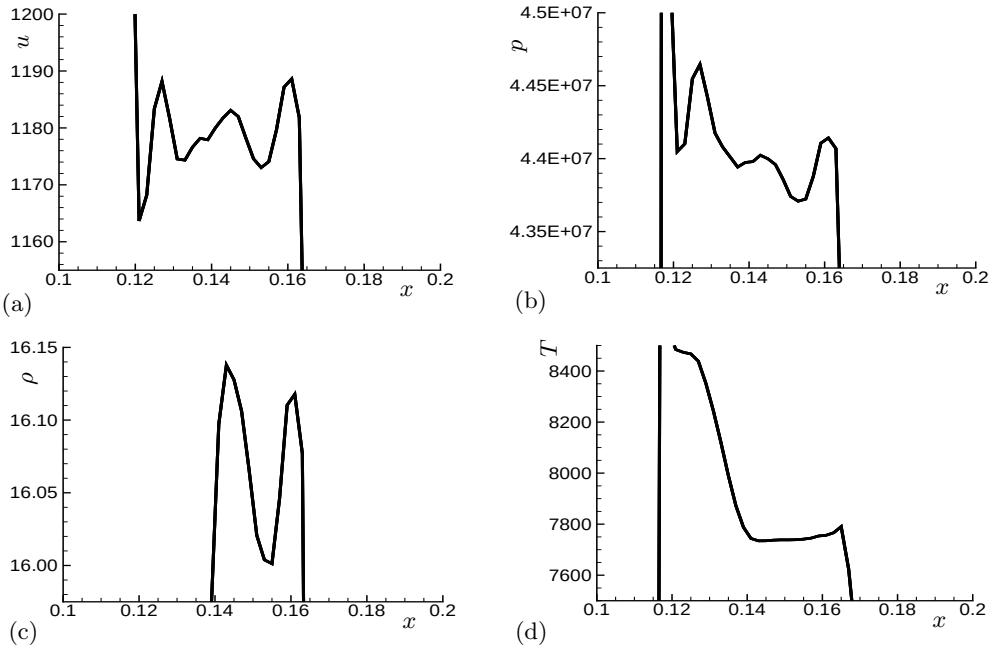

FIGURE 7. Case III: disturbance evolution for a entropic disturbance after the shock. (a) velocity u, (b) pressure, (c) density ρ, (d) temperature T.

purposes, the ideal gas case was presented, which showed a decrease in disturbance amplitude and wavelength downstream of the shock. With equilibrium chemistry, the decrease was even more pronounced. In the third case, the effect of the non-equilibrium chemistry was investigated and found to be adverse, leading to an increase both in amplitude and wavelength.

Chemical non-equilibrium can lead to an increase in disturbance levels downstream of a shock. The current work demonstrates the possibility of an enhancement of the instability process in transition where disturbance waves move through small shocks. Additional investigation is required. higher frequencies that lie in the instability range for hypersonic speeds and oblique angles between shock and disturbance.

REFERENCES

Miller, J. H. 2005 Computational Aerothermodynamic datasets for Hypersonic Heat transfer on Reentry Vehicles. *AIAA-2005-5911*.

Lee, S., Lele, S. K., Moin, P. 1993 Direct numerical simulation of isotropic turbulence interacting with a weak shock wave. *J. Fluid Mech.*, **251**,533–562. Including Corrigendum **264**, 373–374, 1994.

Mahesh, K., Lee, S., Lele, S. K., Moin, P. 1995 The Interaction of an isotropic field of acoustic waves with a shock wave. *J. Fluid Mech.*, **300**, 383–407.

Mahesh, K., Lele, S. K., Moin, P. 1997 The influence of entropy fluctuations on the interaction of turbulence with a shock wave. *J. Fluid Mech.*, **334**, 353–379.

Lee, S., Lele, S. K., Moin, P. 1997 Interaction of isotropic turbulence with shock waves: effect of shock strength. *J. Fluid Mech.*, **340**, 225–247.

Vos, J. B., Rizzi, A. W., Crojon, A., Chaput, E., Soinne, E. 1998 Recent advances in aerodynamics inside the NSMB (Navier Stokes Multi Block) Consortium. *AIAA-98-0225*.

Vos, J. B., Duquesne, N., Lee, H. J. 1999 Shock wave boundary layer interaction studies using the NSMB flow solver. *Aerothermodynamics for space vehicles, ESA SP-426*, Proceedings of the Third Symposium on Aerothermodynamics for Space Vehicles, 229–236.

Stemmer, C. Hypersonic Transition Investigations In A Flat-Plate Boundary-Layer Flow At M=20. *AIAA-2005-5136*.